Firing Rate BVC Receptive Field

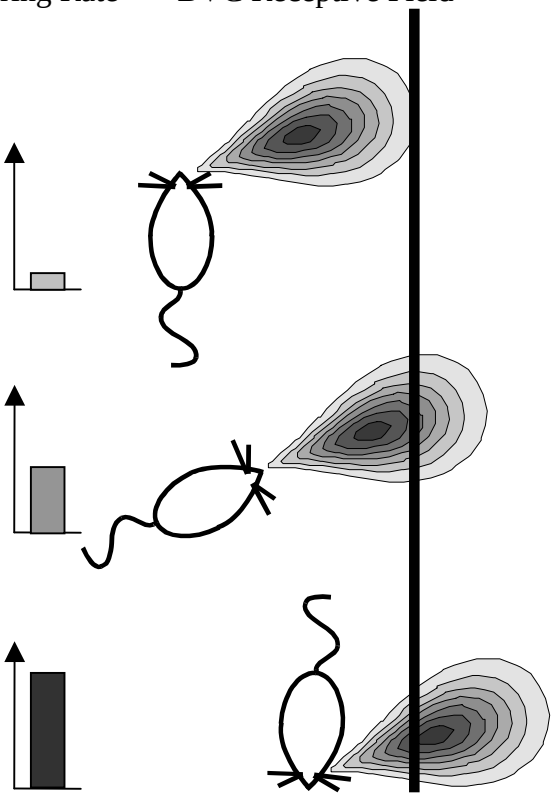

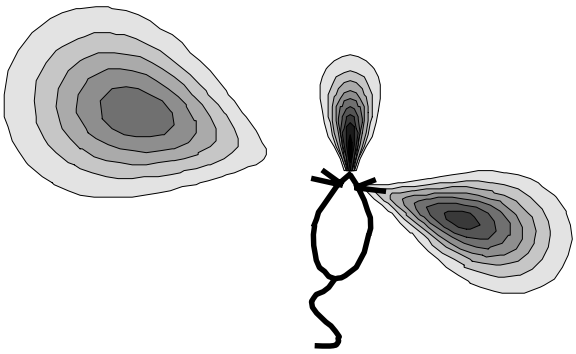

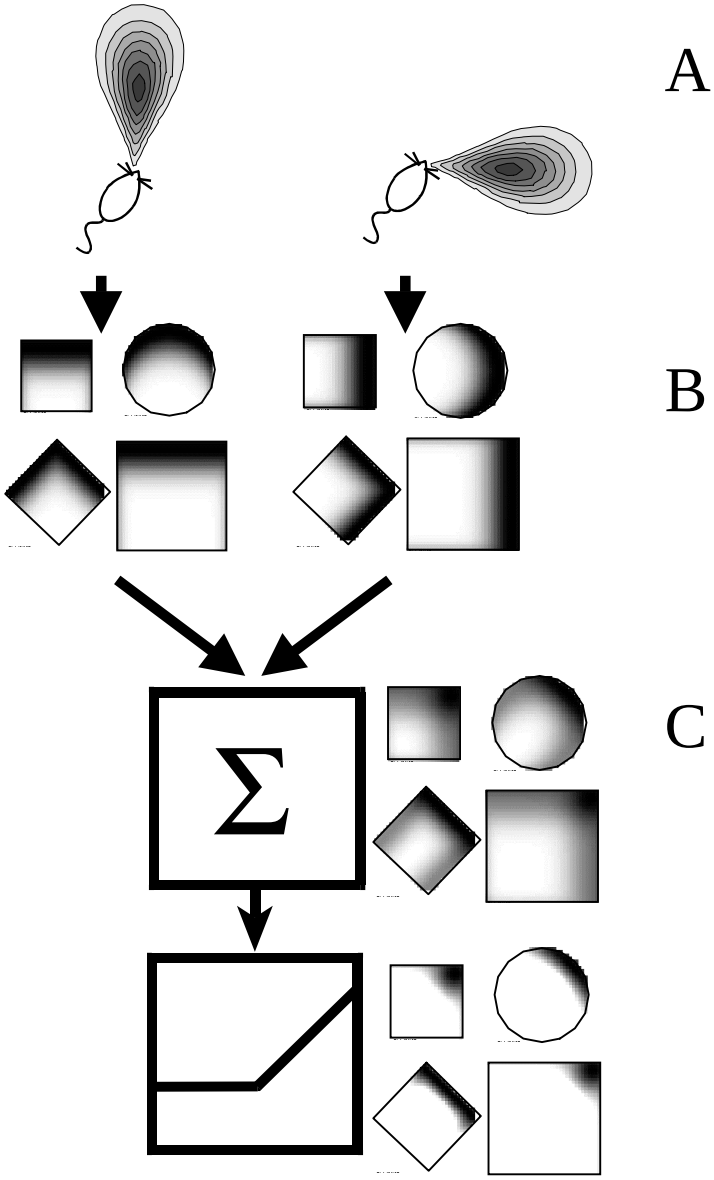
A
B
C
Σ

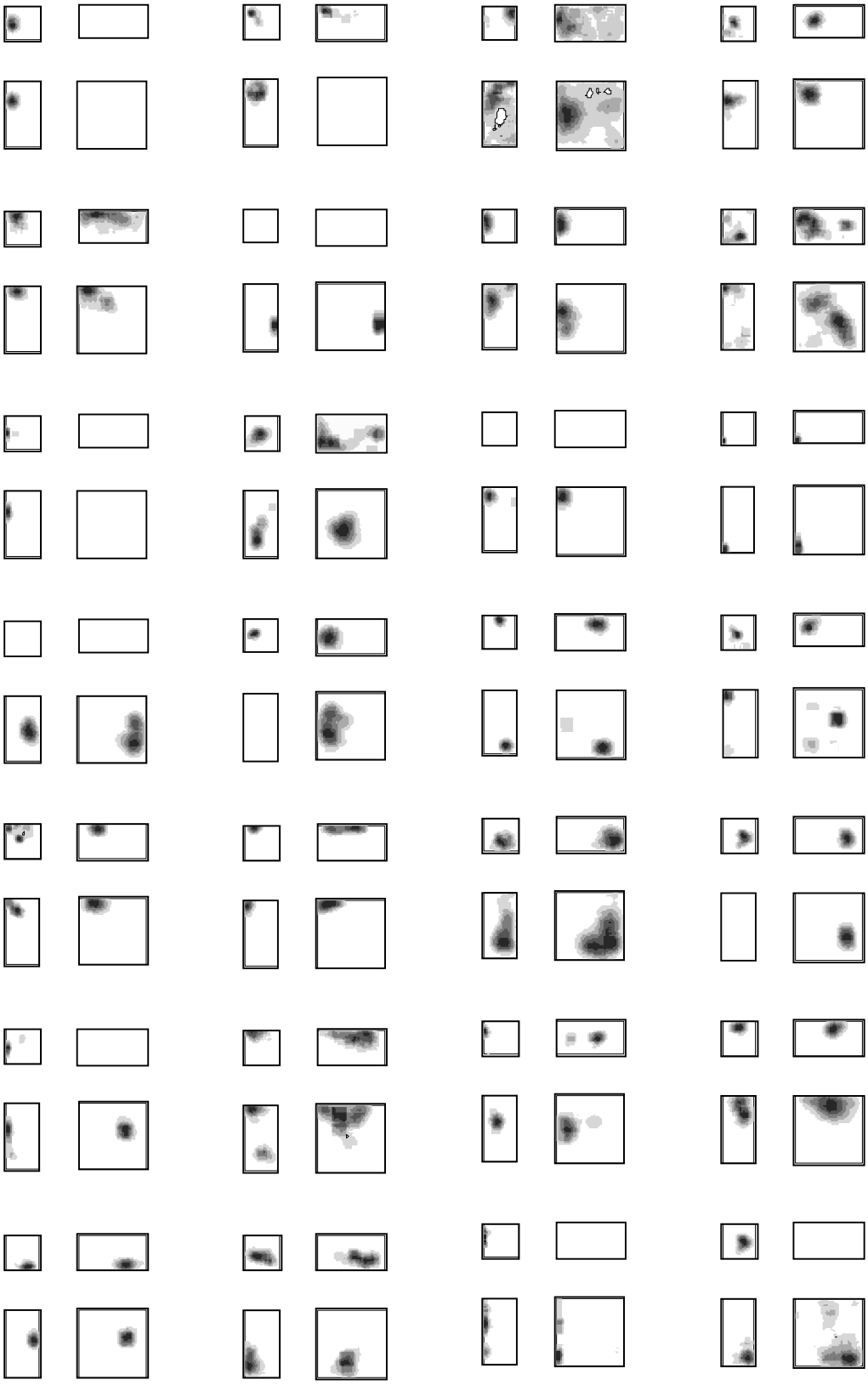

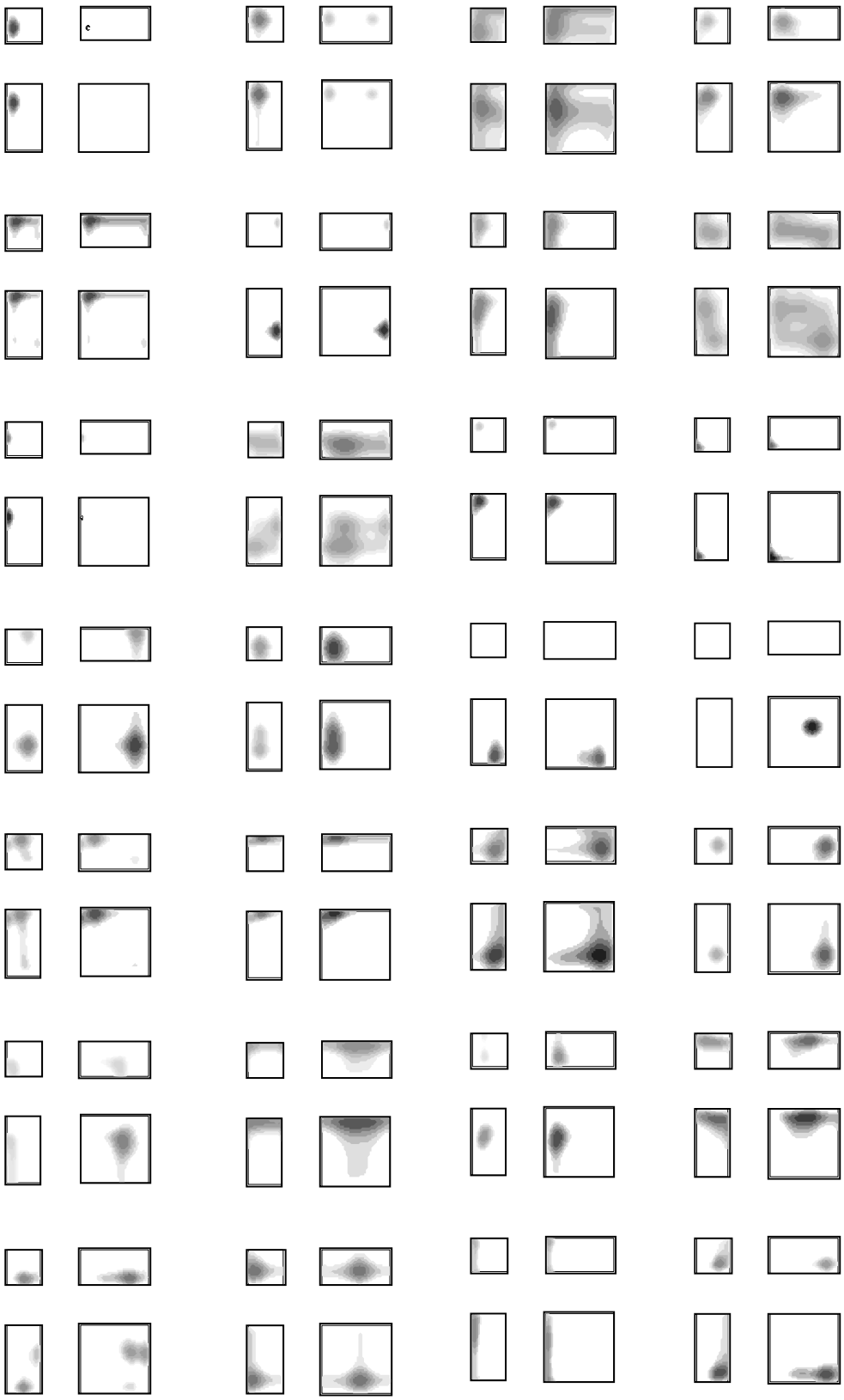

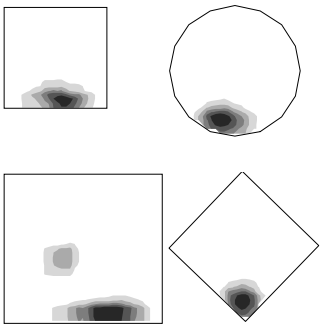

A

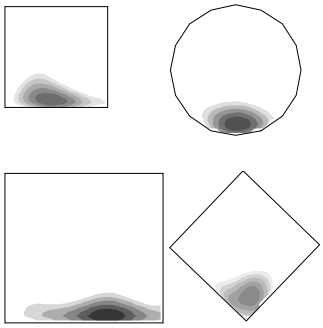

B

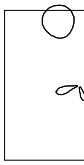

C

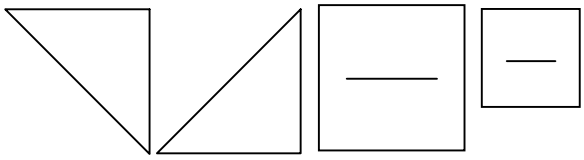

D

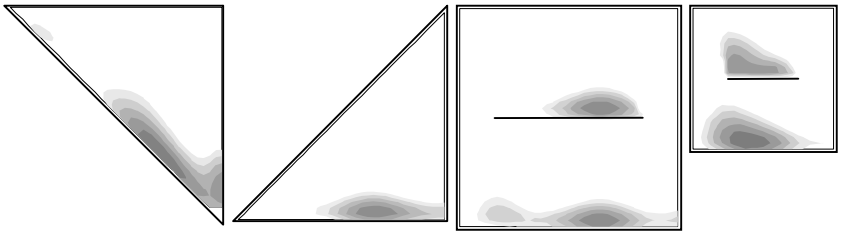

Simulation (Prediction)

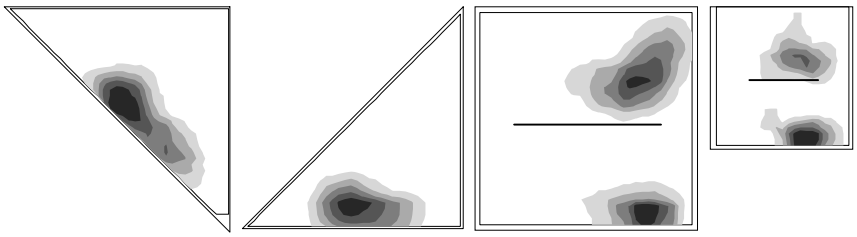

Data (Lever et al, 1999)

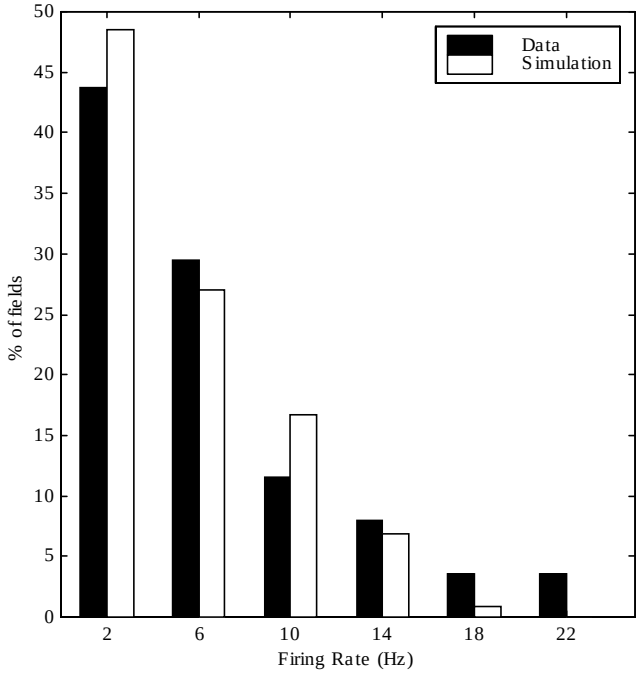
Data
Simulation
% of fields
Firing Rate (Hz)
0
5
10
15
20
25
30
35
40
45
50
2
6
10
14
18
22

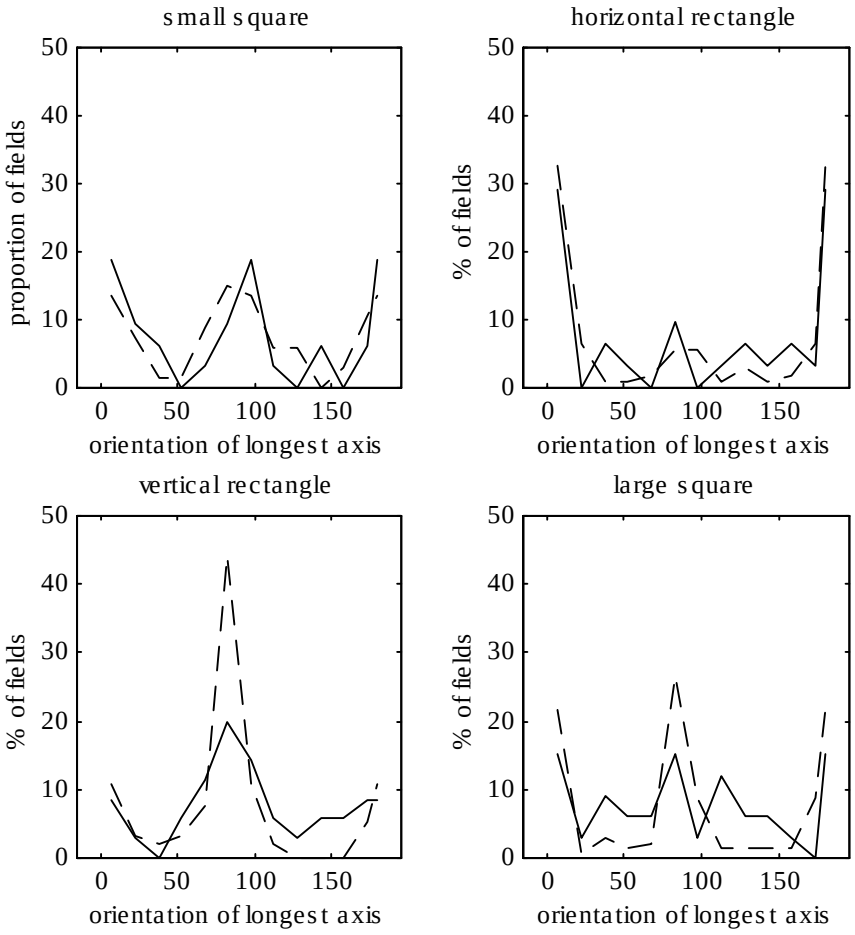
small square
horizontal rectangle
vertical rectangle
large square
proportion of fields
% of fields
orientation of longest axis
0
10
20
30
40
50
0
50
100
150

A

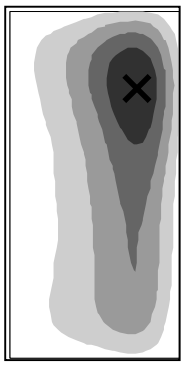

B

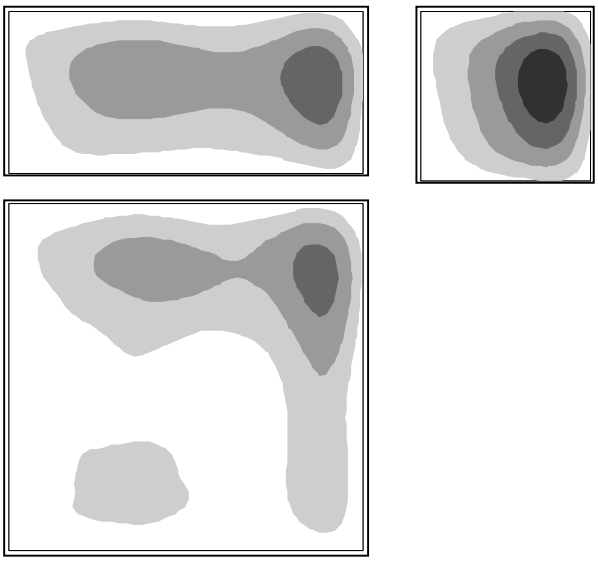

Figure 1. Data from O'Keefe and Burgess (1996a) indicate that place cells respond maximally when the rat is a specific distance away from two or more walls. This suggests inputs to the place cells, boundary vector cells (BVCs), each of which responds to boundaries in the environment at a particular distance and allocentric bearing. Whenever the rat encounters a wall at that distance and direction, the BVC's firing rate increases.

Figure 2. The receptive fields of the BVCs are the product of Gaussian functions of distance and direction. The angle subtended by each field (at the rat) is constant. Cells tuned to respond to more distant boundaries have broader tunings to distance than those responding to proximal boundaries. Each place cell receives input from a number of BVCs. The shading indicates the relative level of activation produced by wall segments intersecting each of the three receptive fields (*g*, see text). Note that BVC receptive fields tuned to respond maximally to more distant walls produce less activation at their peaks than those tuned to shorter distances.

Figure 3. A) BVC receptive fields (shown relative to rat, independent of heading). Not to scale with the environments. B) Corresponding BVC firing fields (in a variety of environments -- a small square, a circle, a large square and a diamond). C) A place cell's firing rate is modelled as the thresholded sum of two or more BVC firing fields. The sum of the two BVCs in B is shown above, and the result of applying a threshold-linear transfer function is shown below.

Figure 4A. Data from 28 place fields reported by O'Keefe and Burgess (1996a), shown for comparison with simulated cell firing rates maps shown in figure 4B. The shading indicates the rate of firing, which has been normalised within each environment, so that the peak firing rate corresponds to the darkest shading. As in O'Keefe and Burgess (1996a), fields with peak firing rates less than 1Hz are not shown, and the cell was treated as if it had zero firing rate in these environments. Pretraining of the rat occurred in the vertical rectangle, except for cells shown in the rightmost column in which pretraining occurred in the horizontal rectangle.

Figure 4B. Firing rate maps of 28 simulated place cells with 2-4 BVC inputs chosen to fit the corresponding experimental data shown in figure 4A. These plots show the actual fitted values for $F(\underline{x})$ using the same shading scale as figure 4A.

Figure 5. A) Place field data (Lever et al, 1999) B) Place field simulation. C) Fitted BVC receptive fields (shown as contours at half maximum). The large box (93cm x 93cm) is shown for scale. D) Novel environments for which firing will be predicted (to scale). The BVCs shown in C are used to predict the firing pattern that will be observed in these environments (see figure 6). The shading scheme for real and simulated firing maps is as in figures 4A and 4B respectively.

Figure 6. Prediction of the behaviour of the place cell fitted in figure 5 in four novel environments. The actual recordings for that cell are shown below for comparison. The shading scheme used for simulated and real firing maps is as used in figures 4B and 4A respectively.

Figure 7. Across all environments, the model shows a similar distribution of peak firing rates to that observed experimentally. The simulated peak firing rate for each environment is calculated by scaling the summed thresholded BVC inputs (see text) by a factor such that the median firing rate of real and simulated cells is equal (4.85Hz).

Figure 8. Orientation of place fields in real (solid lines -- data from O'Keefe and Burgess, 1996a) and simulated place fields (dashed lines). The shape of each field was defined as a region enclosed by a contour drawn at half maximum firing rate. For each such region, the axis of greatest extent was measured to the nearest 7.5º, and plotted here in 15º bins (0-15º, 15-30º etc.). The rectangular boxes in which the fields were recorded/simulated had walls orientated at 0º and 90º. Both real and simulated fields show a tendency for the longest axis to be parallel to the walls, especially in rectangular boxes.

Figure 9. Behavioural predictions. If the hippocampal representation of space is used to guide behaviour, an animal searching for an object previously seen at location X would be expected to focus its search on locations with similar representations in the place cells. A shows the similarity of the place cell representation at all locations within a rectangular environment with the place cell representation at location X. We would predict the locus of search for an object found at X to be a monotonic function of the similarity field shown. What would be the locus of search if environment A changed shape after the object was found? B shows the similarity of the place cell representation of locations in three different shaped environments to the place cell representation of location X in environment A. We predict the locus of search to be a monotonic function of these similarity fields. *Details*: the similarity between the place cell representations of two places is expressed as the dot product of the vectors of the cells' firing rates at the two places (black=maximum, white=0). We simulated 289 place cells each with 10 randomly chosen BVC inputs (as described in "Statistical Properties of Populations of Place Cells") so that 100 of them were active at location X (and so contributed to the dot products).